Supplementary Materials for

Theoretical Insights on Tunable Optoelectronics and Charge Mobilities in Cyano-Perylenediimides: Interplays between -CN Numbers and Positions

Raka Ahmed and Arun K Manna*

Department of Chemistry and Center for Atomic, Molecular and Optical Sciences & Technologies, Indian Institute of Technology Tirupati, Tirupati, A.P 517506

*Corresponding Author E-mail: arun@iittp.ac.in

Table S1: Molecular dipole moments (μ, in Debye), HOMO (H) and LUMO (L) energies along with Mülliken electronegativity $\chi = -\frac{1}{2}(E_H + E_L)$ calculated using OT-RSH/6-311G (d, p) are listed in eV unit and also the percentage contribution of -CN to the HOMO and the LUMO orbitals of different PDI monomers considered in this study.

Monomers	$\boldsymbol{\mu}$	$\boldsymbol{E_H}$	$\boldsymbol{E_L}$	$\boldsymbol{\chi}$	**% of -CN Group**	
					HOMO	**LUMO**
Pristine-PDI	0.00	-7.78	-2.34	5.06	0	0
PDI-$(CN)_2$-a	1.98	-8.37	-3.00	5.69	4.32	4.48
PDI-$(CN)_2$-b	0.00	-8.34	-3.00	5.67	0.57	2.51
PDI-$(CN)_4$-a	0.00	-8.87	-3.60	6.23	1.23	4.49
PDI-$(CN)_4$-b	4.05	-8.83	-3.49	6.16	6.35	4.59

Table S2: Calculated HOMO (E_H), LUMO (E_L) energies and the HOMO-LUMO gap (ΔE_{H-L}) for all the PDI monomers using OT-RSH, OT-SRSH and OT-SRSH+PCM method with 6-311G (d, p) basis set. All energies are in eV.

Monomer	**OT-RSH**			**OT-SRSH**			**OT-SRSH+PCM**		
	$\boldsymbol{E_H}$	$\boldsymbol{E_L}$	$\boldsymbol{\Delta E_{H-L}}$	$\boldsymbol{E_H}$	$\boldsymbol{E_L}$	$\boldsymbol{\Delta E_{H-L}}$	$\boldsymbol{E_H}$	$\boldsymbol{E_L}$	$\boldsymbol{\Delta E_{H-L}}$
Pristine-PDI	-7.78	-2.34	5.44	-4.68	-1.89	2.79	-4.52	-1.74	2.78
PDI-$(CN)_2$-a	-8.37	-3.00	5.37	-5.41	-2.59	2.82	-5.14	-2.32	2.82
PDI-$(CN)_2$-b	-8.34	-3.00	5.34	-5.34	-2.58	2.76	-4.99	-2.27	2.72
PDI-$(CN)_4$-a	-8.87	-3.60	5.27	-6.05	-3.23	2.82	-5.55	-2.78	2.77
PDI-$(CN)_4$-b	-8.83	-3.49	5.34	-5.90	-3.11	2.79	-5.50	-2.71	2.79

Table S3: Isotropic polarizability (α_{iso}), molecular volume (V_m) and scalar dielectric constant (ε_s) for all gas-phase PDI molecules calculated using OT-RSH/6-311++G (d, p). The first

singlet excited-state S_1 (optically bright and intense one characterized by large oscillator strength given in parentheses) calculated with different functionals (OT-RSH, OT-SRSH and OT-SRSH+PCM) are also tabulated for all functional PDI monomers.

Molecule	$\boldsymbol{\alpha_{iso}}$ **(a.u.)**	$\boldsymbol{V_m}$ **(a.u.)**	$\boldsymbol{\varepsilon_s}$	$\boldsymbol{S_1}$**State Energy (eV)**		
				OT-RSH	**OT-SRSH**	**OT-SRSH + PCM**
Pristine-PDI	348.263	2770.009	4.34	2.77 (0.70)	2.54 (0.62)	2.35 (0.92)
PDI-$(CN)_2$-a	379.948	3096.227	4.17	2.71 (0.57)	2.50 (0.50)	2.34 (0.75)
PDI-$(CN)_2$-b	388.220	2988.549	4.58	2.75 (0.65)	2.53 (0.58)	2.33 (0.87)
PDI-$(CN)_4$-a	428.959	3436.355	4.29	2.75 (0.62)	2.54 (0.55)	2.33 (0.83)
PDI-$(CN)_4$-b	415.412	3187.883	4.61	2.72 (0.51)	2.49 (0.45)	2.35 (0.70)

Table S4: The calculated 0-0 energy ($E_{0-0} = E_{vert.} - \Delta ZPVE - \lambda_{S_1}$), the difference in ZPVE ($\Delta ZPVE$) and the S_1 state relaxation energy (λ_{S_1}) for all PDI monomers calculated in the condensed-phase using OT-RSH+PCM and OT-SRSH+PCM. The $E_{vert.}$ indicates the vertical excitation energy for the S_1 state. The ZPVE energies for S_0 and S_1 states are obtained using ωB97X-D+PCM. All energies are listed in eV.

Molecule	$\boldsymbol{E_{0-0}}$		$\boldsymbol{\Delta ZPVE = E(S_0) - E(S_1)}$	$\boldsymbol{\lambda_{S_1}}$	
	OT-RSH +PCM	**OT-SRSH +PCM**		**OT-RSH +PCM**	**OT-SRSH +PCM**
Pristine-PDI	2.28	2.14	0.07	0.21	0.13
PDI-$(CN)_2$-a	2.28	2.14	0.05	0.22	0.14
PDI-$(CN)_2$-b	2.25	2.12	0.08	0.21	0.12
PDI-$(CN)_4$-a	2.26	2.13	0.08	0.20	0.12
PDI-$(CN)_4$-b	2.30	2.16	0.05	0.22	0.14

Table S5: Calculated HOMO (E_H), LUMO (E_L) energies and the HOMO-LUMO gap (ΔE_{H-L}) for all functional PDI dimers using OT-RSH/6-311G (d, p). Low-lying four singlet excited-state energies are also provided. Oscillator strengths are listed within the bracket. All energies are in eV.

Dimers	$\boldsymbol{E_H}$	$\boldsymbol{E_L}$	$\boldsymbol{\Delta E_{H-L}}$	**S₁**	**S₂**	**S₃**	**S₄**
Pristine-PDI	-7.64	-2.62	5.02	2.39 (0.02)	2.61 (0.05)	2.77 (0.03)	2.81 (0.86)

PDI-$(CN)_2$-a (d1)	-8.33	-3.38	4.95	2.41 (0.02)	2.53 (0.04)	2.67 (0.21)	2.73 (0.49)
PDI-$(CN)_2$-a (d2)	-8.19	-3.38	4.81	2.26 (0.04)	2.54 (0.10)	2.71 (0.49)	2.82 (0.07)
PDI-$(CN)_2$-b (d1)	-8.30	-3.44	4.86	2.32 (0.02)	2.58 (0.07)	2.80 (0.72)	2.82 (0.05)
PDI-$(CN)_2$-b (d2)	-8.38	-3.42	4.96	2.43 (0.02)	2.57 (0.07)	2.69 (0.02)	2.81 (0.77)
PDI-$(CN)_4$-a	-8.93	-4.14	4.79	2.32 (0.02)	2.57 (0.06)	2.79 (0.69)	2.83 (0.02)
PDI-$(CN)_4$-b (d1)	-8.71	-3.83	4.88	2.49 (0.03)	2.50 (0.06)	2.65 (0.58)	2.75 (0.01)
PDI-$(CN)_4$-b (d2)	-8.87	-4.08	4.79	2.37 (0.02)	2.49 (0.13)	2.63 (0.01)	2.67 (0.49)

Table S6: Four lowest singlet excite-state energies ($E_{S_n}, n = 1-4$) with the major contribution from occupied → unoccupied FMOs replacement and the charge-transfer number (q_{CT}) for all functional PDI dimers calculated in the gas-phase using OT-RSH and also in the condensed-phase using OT-SRSH+PCM with 6-311G (d, p) basis set for all atoms. Oscillator strengths are listed within the bracket. H and L represent HOMO and HOMO, respectively. All energies are in eV.

PDI Dimers	**Ex. State**	**Gas-Phase (OT-RSH)**			**Condensed-Phase (OT-SRSH+PCM)**		
	S_n	E_{S_n} **(eV)**	**Major Contribution**	q_{CT}	E_{S_n} **(eV)**	**Major Contribution**	q_{CT}
Pristine-PDI	S_1	2.39 (0.02)	H→L (0.70)	0.39	2.04 (0.02)	H→L (0.70)	0.65
	S_2	2.61 (0.05)	H→L+1 (0.60); H-1→L (0.37)	0.92	2.16 (0.02)	H→L+1 (0.56); H-1→L (0.43)	0.95
	S_3	2.77 (0.03)	H-1→L+1 (0.70)	0.61	2.42 (0.07)	H-1→L+1 (0.70)	0.35
	S_4	2.81 (0.86)	H-1→L (0.59); H→L+1 (0.37)	0.07	2.45 (1.42)	H-1→L (0.56); H→L+1 (0.43)	0.05
PDI-$(CN)_2$-a (d1)	S_1	2.41 (0.02)	H→L (0.63)	0.53	2.09 (0.02)	H→L (0.66)	0.84
	S_2	2.53 (0.04)	H→L+1 (0.47); H-1→L (0.43)	0.52	2.16 (0.04)	H→L+1 (0.59); H-1→L+1 (0.34)	0.85
	S_3	2.67 (0.21)	H-1→L+1 (0.45); H-1→L (0.40)	0.63	2.30 (0.06)	H-1→L+1 (0.49); H-1→L (0.47)	0.23

	S_4	2.74 (0.50)	H-1→L+1 (0.53); H-1→L (0.36)	0.30	2.40 (1.12)	H-1→L (0.44); H-1→L+1 (0.38)	0.07
PDI-$(CN)_2$-a (d2)	S_1	2.26 (0.04)	H→L (0.70)	0.45	1.94 (0.04)	H→L (0.70)	0.60
	S_2	2.54 (0.10)	H→L+1 (0.66)	0.81	2.14 (0.07)	H→L+1 (0.61); H-1→L (0.35)	0.91
	S_3	2.71 (0.49)	H-1→L (0.65)	0.18	2.40 (0.93)	H-1→L (0.61); H→L+1 (0.35)	0.10
	S_4	2.82 (0.07)	H-1→L+1 (0.70)	0.55	2.50 (0.14)	H-1→L+1 (0.70)	0.40
PDI-$(CN)_2$-b (d1)	S_1	2.32 (0.02)	H→L (0.70)	0.45	1.97 (0.03)	H→L (0.70)	0.61
	S_2	2.58 (0.07)	H→L+1 (0.62); H-1→L (0.33)	0.88	2.15 (0.04)	H→L+1 (0.58); H-1→L (0.40)	0.94
	S_3	2.80 (0.72)	H-1→L (0.61); H→L+1 (0.32)	0.13	2.43 (1.28)	H-1→L (0.58); H→L+1 (0.40)	0.06
	S_4	2.82 (0.05)	H-1→L+1 (0.69)	0.53	2.49 (0.07)	H-1→L+1 (0.70)	0.38
PDI-$(CN)_2$-b (d2)	S_1	2.43 (0.02)	H→L (0.70)	0.40	2.08 (0.01)	H→L (0.69)	0.70
	S_2	2.57 (0.07)	H→L+1 (0.62); H-1→L (0.32)	0.89	2.15 (0.05)	H→L+1 (0.59); H-1→L (0.39)	0.93
	S_3	2.69 (0.02)	H-1→L+1 (0.70)	0.59	2.37 (0.05)	H-1→L+1 (0.69)	0.30
	S_4	2.81 (0.77)	H-1→L (0.62); H→L+1 (0.32)	0.11	2.44 (1.30)	H-1→L (0.59); H→L+1 (0.39)	0.06
PDI-$(CN)_4$-a	S_1	2.32 (0.02)	H→L (0.70)	0.46	1.99 (0.02)	H→L (0.70)	0.61
	S_2	2.57 (0.06)	H→L+1 (0.61); H-1→L (0.34)	0.90	2.19 (0.03)	H→L+1 (0.57); H-1→L (0.42)	0.95
	S_3	2.79 (0.69)	H-1→L (0.61); H→L+1 (0.34)	0.10	2.45 (1.21)	H-1→L (0.57); H→L+1 (0.41)	0.05
	S_4	2.83 (0.02)	H-1→L+1 (0.70)	0.54	2.52 (0.06)	H-1→L+1 (0.70)	0.39
PDI-$(CN)_4$-b (d1)	S_1	2.49 (0.03)	H→L+1 (0.47); H→L (0.40); H-1 → L (0.32)	0.50	2.12 (0.00)	H→L (0.66)	0.96
	S_2	2.50 (0.06)	H→L (0.57); H→L+1 (0.32)	0.48	2.24 (0.04)	H-1→L+1 (0.66)	0.79
	S_3	2.65 (0.58)	H-1→L (0.55); H→L+1 (0.41)	0.03	2.27 (0.19)	H→L+1 (0.54); H-1→L (0.35)	0.21
	S_4	2.75 (0.01)	H-1→L+1 (0.67)	0.95	2.36 (0.92)	H-1→L (0.61); H→L+1 (0.31)	0.04
PDI-$(CN)_4$-b (d2)	S_1	2.37 (0.02)	H→L (0.70)	0.39	2.08 (0.02)	H→L (0.69)	0.68
	S_2	2.49 (0.13)	H-1→L (0.66)	0.77	2.13 (0.10)	H-1→L (0.63); H→L+1 (0.32)	0.87
	S_3	2.63 (0.01)	H-1→L+1 (0.70)	0.61	2.35 (0.05)	H-1→L+1 (0.69)	0.32

	S_4	2.67 (0.49)	H→L+1 (0.66)	0.22	2.37 (0.93)	H→L+1 (0.63); H-1→L (0.32)	0.13

Table S7: Singlet excited-state energies for the S_1 and intense one (in eV) of all PDI dimers calculated using OT-RSH, OT-SRSH and OT-SRSH+PCM methods with 6-311G (d, p) basis set for all atoms.

Dimers	**OT-RSH**		**OT-SRSH**		**OT-SRSH+PCM**	
	S_1	**Intense**	S_1	**Intense**	S_1	**Intense**
Pristine-PDI	2.39 (0.02)	2.81 (0.86)	2.07 (0.01)	2.64 (0.81)	2.04 (0.02)	2.45 (1.42)
PDI-$(CN)_2$-a (d1)	2.41 (0.02)	2.73 (0.49)	2.04 (0.00)	2.55 (0.64)	2.09 (0.02)	2.40 (1.12)
PDI-$(CN)_2$-a (d2)	2.26 (0.04)	2.71 (0.49)	1.97 (0.02)	2.53 (0.52)	1.94 (0.04)	2.40 (0.93)
PDI-$(CN)_2$-b (d1)	2.32 (0.02)	2.80 (0.72)	2.02 (0.01)	2.63 (0.71)	1.97 (0.03)	2.43 (1.27)
PDI-$(CN)_2$-b (d2)	2.43 (0.02)	2.81 (0.77)	2.12 (0.01)	2.63 (0.74)	2.08 (0.01)	2.44 (1.30)
PDI-$(CN)_4$-a	2.32 (0.02)	2.79 (0.69)	2.05 (0.01)	2.63 (0.66)	1.99 (0.02)	2.45 (1.21)
PDI-$(CN)_4$-b (d1)	2.49 (0.03)	2.65 (0.58)	2.05 (0.00)	2.48 (0.53)	2.12 (0.00)	2.36 (0.92)
PDI-$(CN)_4$-b (d2)	2.37 (0.02)	2.49 (0.13)	2.10 (0.01)	2.49 (0.53)	2.07 (0.02)	2.37 (0.93)

Table S8: The internal electron (λ_e) and the hole reorganization (λ_h) energies from Nelsen's four-point adiabatic potential (AP) method and also from normal modes (NM) analysis for pristine and cyano-substituted PDIs calculated using ωB97X-D. Relaxation energy contributions from the ground (neutral) state (${\lambda_{e/h}}^{gs}$) and the excited charged (cationic/anionic) state (${\lambda_{e/h}}^{es}$) potential energy surfaces to the total internal reorganization energy (λ_i) are also given in meV unit. Gas-phase values are also provided within the bracket.

Systems	${\lambda_e}^{gs}$	${\lambda_e}^{es}$	λ_e **(AP)**	λ_e **(NM)**	${\lambda_h}^{gs}$	${\lambda_h}^{es}$	λ_h**(AP)**	λ_h **(NM)**
Pristine-PDI	189 (202)	187 (202)	376 (404)	382 (408)	109 (125)	109 (122)	218 (247)	221 (253)
PDI-$(CN)_2$-a	175 (189)	176 (190)	351 (379)	348 (374)	118 (131)	117 (129)	235 (260)	240 (265)
PDI-$(CN)_2$-b	177 (189)	175 (187)	352 (376)	359 (380)	108 (120)	108 (119)	216 (239)	221 (245)

PDI-$(CN)_4$-a	169 (177)	167 (176)	336 (353)	348 (360)	108 (117)	107 (116)	215 (233)	219 (237)
PDI-$(CN)_4$-b	173 (185)	173 (184)	346 (369)	350 (375)	118 (127)	116 (126)	234 (253)	244 (261)

Table S9: The internal electron (λ_e) and the hole reorganization (λ_h) energies from Nelsen's four-point adiabatic potential (AP) method for pristine and cyano-substituted PDIs calculated using B3LYP-D. Relaxation energy contributions from the ground (neutral) state (${\lambda_{e/h}}^{gs}$) and the excited charged (cationic/anionic) state (${\lambda_{e/h}}^{es}$) potential energy surfaces to the total internal reorganization energy (λ_i) are also given in meV unit. Gas-phase values are also provided within the bracket.

Systems	$\boldsymbol{{\lambda_e}^{gs}}$	$\boldsymbol{{\lambda_e}^{es}}$	$\boldsymbol{\lambda_e}$ **(AP)**	$\boldsymbol{{\lambda_h}^{gs}}$	$\boldsymbol{{\lambda_h}^{es}}$	$\boldsymbol{\lambda_h}$ **(AP)**
Pristine-PDI	119 (129)	120 (133)	239 (262)	68 (79)	67 (78)	135 (157)
PDI-$(CN)_2$-a	112 (123)	115 (127)	227 (250)	69 (80)	69 (79)	138 (159)
PDI-$(CN)_2$-b	107 (118)	108(119)	215 (237)	66 (74)	66 (74)	132 (148)
PDI-$(CN)_4$-a	100 (108)	100 (109)	200 (217)	65 (70)	65 (70)	130 (140)
PDI-$(CN)_4$-b	109 (119)	110 (121)	219 (240)	69 (76)	68 (75)	137 (151)

Table S10: Marcus charge transfer rates for the electron (k_e) and the hole (k_h) transfer calculated at the room temperature (T = 298 K) for all PDIs considered in the present study adopting the internal reorganization energy λ_i (left) and also the total reorganization energy $\lambda = \lambda_i + \lambda_o$ (right).

π-Stacked Dimers	**Marcus Rate (s^{-1}) with $\boldsymbol{\lambda = \lambda_i}$**		**Marcus Rate (s^{-1}) with $\boldsymbol{\lambda = \lambda_i + \lambda_o}$**	
	$\boldsymbol{k_e}$	$\boldsymbol{k_h}$	$\boldsymbol{k_e}$	$\boldsymbol{k_h}$
Pristine-PDI	2.37×10^{12}	6.10×10^{13}	2.12×10^{12}	5.41×10^{13}
PDI-$(CN)_2$-a (d1)	8.37×10^{7}	2.19×10^{13}	7.49×10^{7}	1.95×10^{13}
PDI-$(CN)_2$-a (d2)	1.03×10^{13}	1.32×10^{14}	9.18×10^{12}	1.18×10^{14}
PDI-$(CN)_2$-b (d1)	7.45×10^{12}	1.29×10^{14}	6.67×10^{12}	1.15×10^{14}
PDI-$(CN)_2$-b (d2)	3.68×10^{11}	5.74×10^{13}	3.29×10^{11}	5.09×10^{13}
PDI-$(CN)_4$-a	1.01×10^{13}	1.29×10^{14}	9.07×10^{12}	1.15×10^{14}
PDI-$(CN)_4$-b (d1)	3.93×10^{11}	1.74×10^{11}	3.52×10^{11}	1.55×10^{11}
PDI-$(CN)_4$-b (d2)	2.24×10^{13}	6.58×10^{12}	2.01×10^{13}	5.85×10^{12}

Table S11: Calculated electron (μ_e) and hole (μ_h) mobilities obtained at room temperature (T = 298 K) for all PDIs studied here adopting the internal reorganization energy λ_i (left) and also with the total reorganization energy λ (right).

π-Stacked Dimers	**Carriers Mobility with $\lambda = \lambda_i$ [cm^2/(V-s)]**		**Carriers Mobility with $\lambda = \lambda_i + \lambda_o$ [cm^2/(V-s)]**	
	μ_e	μ_h	μ_e	μ_h
Pristine-PDI	0.10	2.70	0.09	2.39
PDI-$(CN)_2$-a (d1)	3.84×10^{-6}	1.01	3.43×10^{-6}	0.89
PDI-$(CN)_2$-a (d2)	0.47	6.14	0.43	5.45
PDI-$(CN)_2$-b (d1)	0.33	5.67	0.29	5.03
PDI-$(CN)_2$-b (d2)	1.66×10^{-2}	2.58	1.48×10^{-2}	2.29
PDI-$(CN)_4$-a	0.44	5.61	0.39	4.97
PDI-$(CN)_4$-b (d1)	2.68×10^{-2}	1.19×10^{-2}	2.39×10^{-2}	0.01
PDI-$(CN)_4$-b (d2)	1.18	0.35	1.05	0.31

Table S12: Marcus charge transfer rates ($k_{e/h}$) and the electron (μ_e) and the hole (μ_h) mobilities calculated at room temperature (T = 298 K) for the fully optimized PDI and also the slipped stacked (ss-PDI) and the rotated sandwich (rs-PDI) dimer structures extracted from two different crystal structures considered in the present study. Charge hopping distance (r), electronic coupling (V) and internal reorganization energies (λ_i) for each dimer are also listed. Rates and charge mobilities listed within the bracket are calculated using the total reorganization energy (λ).

Dimer	**r (Å)**	**λ_i (meV)**		**V (meV)**		**Marcus Rate (s^{-1})**		**Mobility (cm^2/V.s)**	
		λ_e	λ_h	V_e	V_h	k_e	k_h	μ_e	μ_h
PDI	3.37	376	218	58	119	2.4×10^{12} (2.1×10^{12})	6.1×10^{13} (5.4×10^{13})	0.10 (0.09)	2.7 (2.39)
ss-PDI	4.68	376	218	40	186	1.13×10^{12} (1.01×10^{12})	1.49×10^{14} (1.32×10^{14})	0.10 (0.09)	12.72 (11.28)
rs-PDI	3.66	376	218	109	95	8.37×10^{12} (7.50×10^{12})	3.89×10^{13} (3.45×10^{13})	0.44 (0.39)	2.03 (1.80)

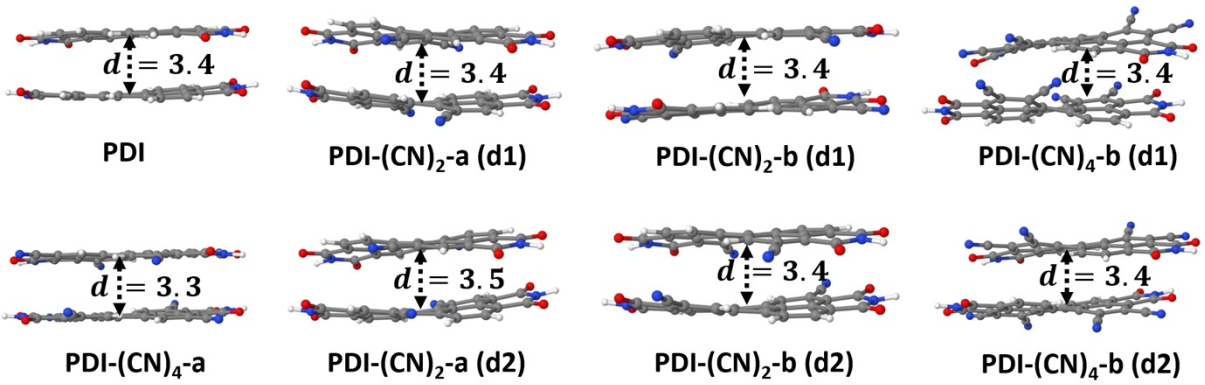

Figure S1: Side-view of all PDI dimer geometries optimized at ωB97X-D/6-311G (d, p) level of theory. H, C, N and O are indicated by white, grey, blue and red colour balls, respectively. Stacking distances (d) are also listed in Å.

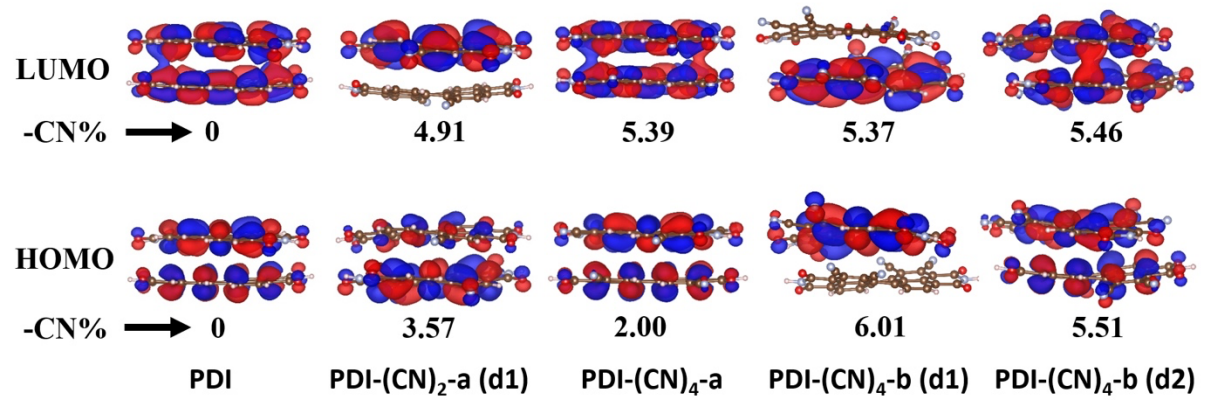

Figure S2: HOMO and LUMO iso-surfaces for the pristine PDI and also for a few functional PDIs calculated using OT-RSH functional in the gas-phase. An iso-value of 0.02 e/Å^3 is used. Percentage of -CN group contributions to the HOMO and the LUMO are also listed.